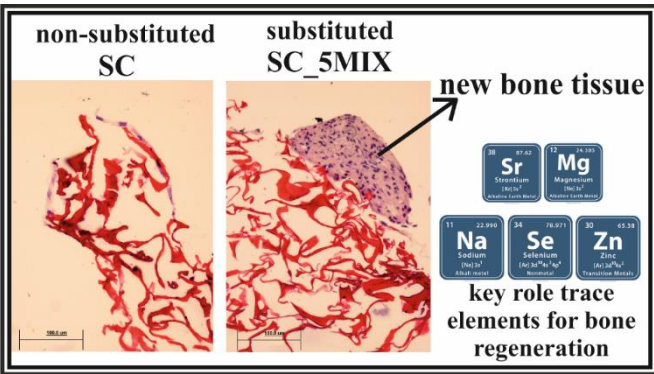


Development of personalized and affordable multi-substituted calcium phosphate-based biomimetic scaffolds for bone regeneration applications

Antonia Ressler*, Erkka J. Frankberg, Roope Ohlsbom, Setareh Zakeri, Markus Hannula, Jari Hyttinen, Martin Schwentenwein, Susanna Miettinen, Erkki Levänen

AffordBoneS

Personalized and affordable multi-substituted calcium phosphate scaffolds



Objective 1/WP1

mCaP precipitation, design of mCaP scaffolds using CAD and scaffold fabrication

scaffold CAD model

substituted mCaP

CeraFab 7500 printer

Collaboration with : **LITHOZ**

The mCaP scaffold properties according to the bone tissue engineering requirements:

- porosity: 50-90 %
- pore size distribution: 100-500 μm
- phase content: hydroxyapatite/tricalcium phosphate
- mechanical properties required for bone augmentation

Objective 2/WP2

In vitro and in vivo osteogenic properties of mCaP scaffolds

In vitro cell culture in static and dynamic conditions

- live/ded assay, Cell Counting
- quantitative reverse transcription polymerase chain reaction
- immunocytochemical and immunohistochemical staining
- histological staining

In vivo characterization during three months in rats

- micro-computed tomography
- inflammation detection

Objective 3/WP3

Obtaining a demonstration of personalized mCaP scaffolds in collaboration with Planmeca

- obtaining CAD design according to the real patient cases provided by Planmeca
- printing customized scaffolds on CaraFab 7500 using previously optimized printing parameters

Collaboration with : **PLANMECA**



Prof. Erkki Levänen



Dr. Erkkka Frankberg



Prof. Susanna Miettinen



LITHOZ
Dr. Martin Schweintenwein



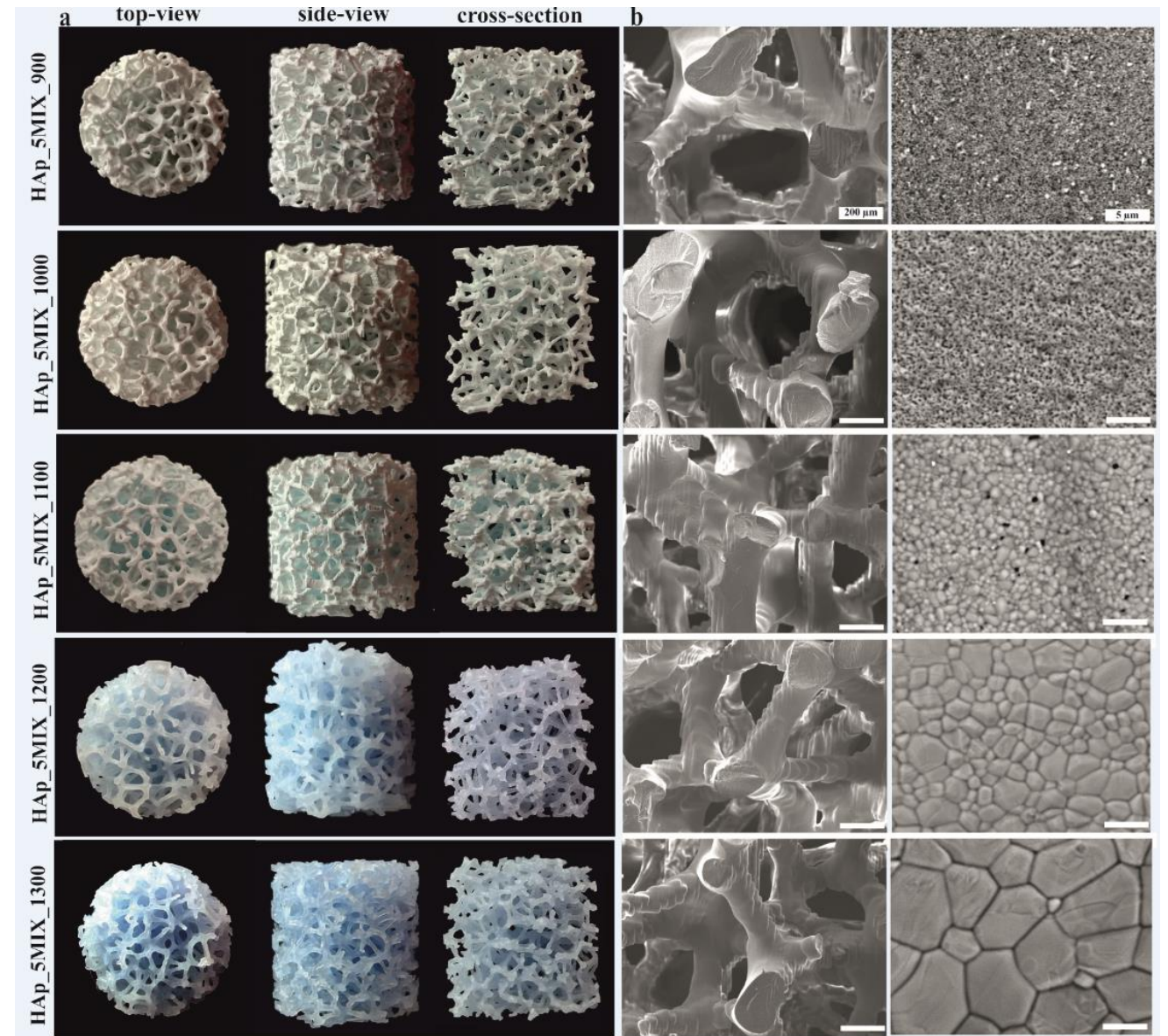
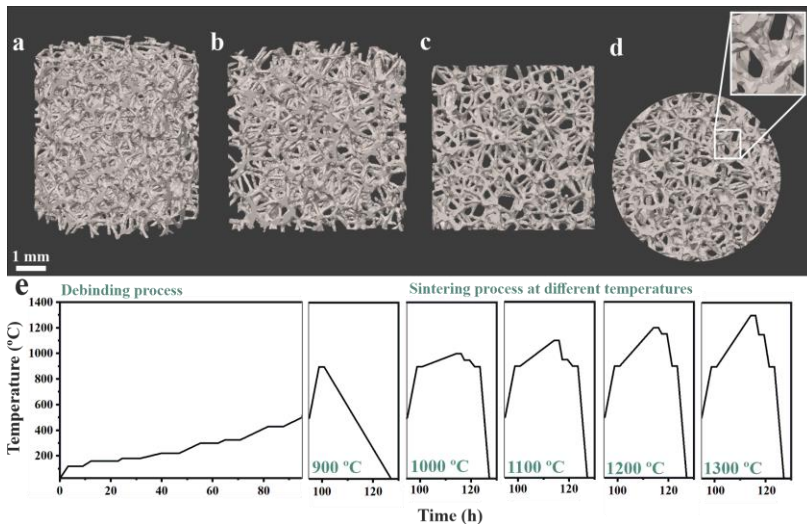
Pontus Degerlund
PLANMECA

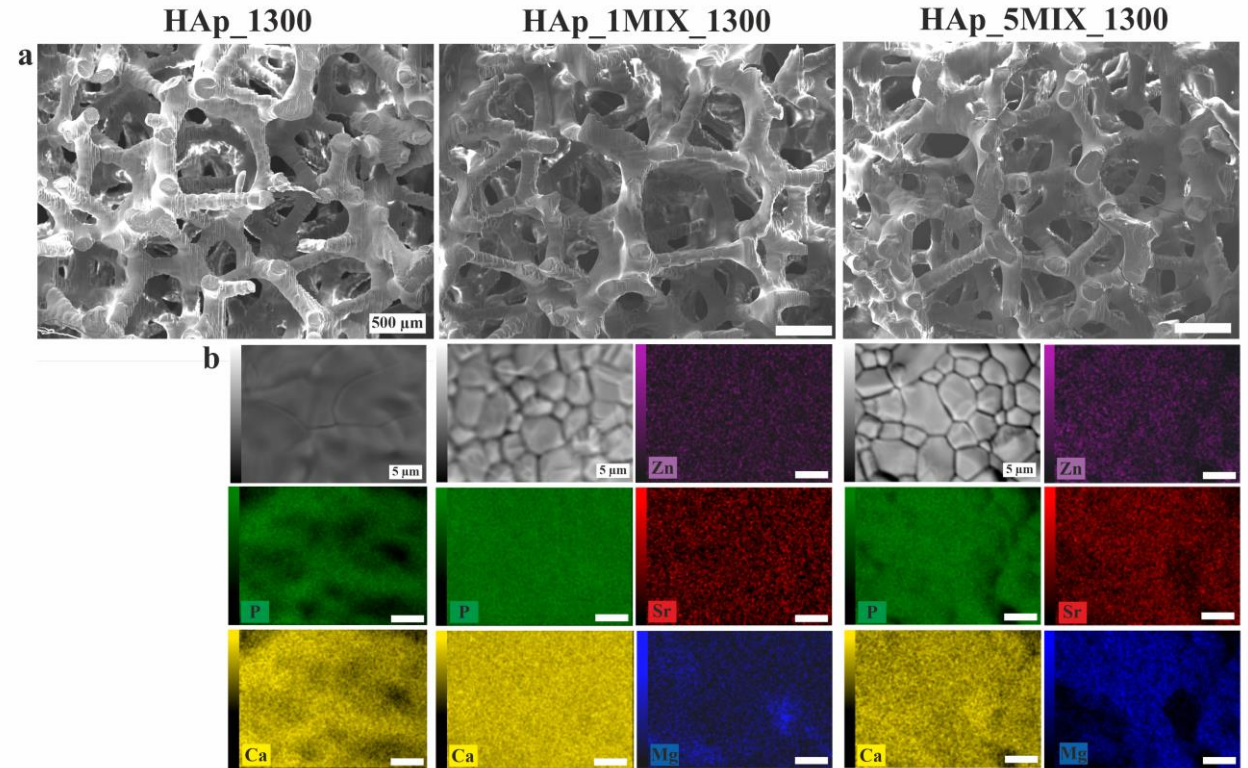
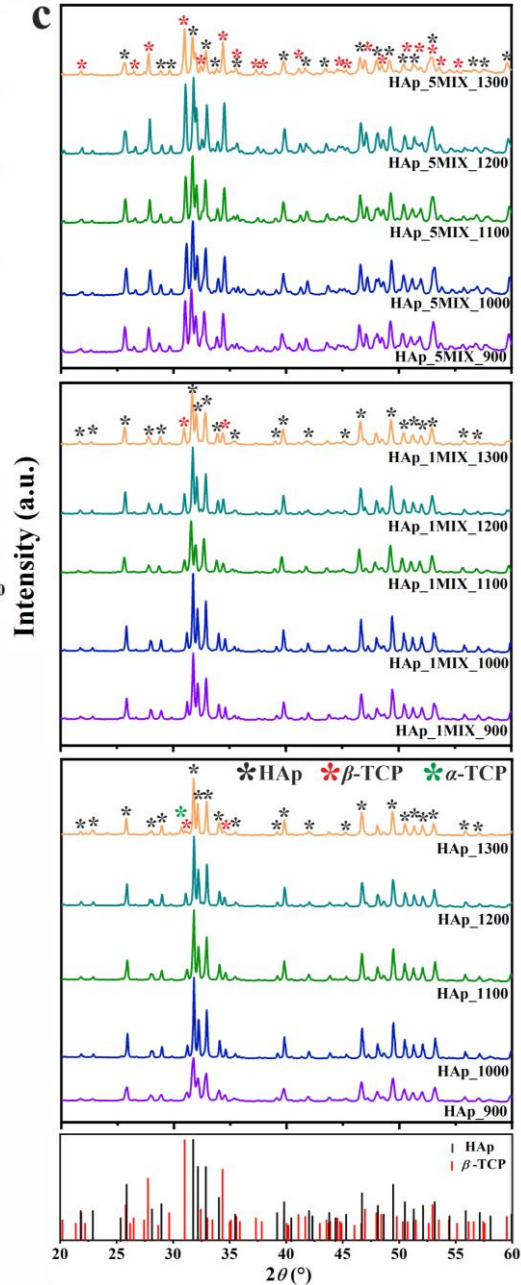
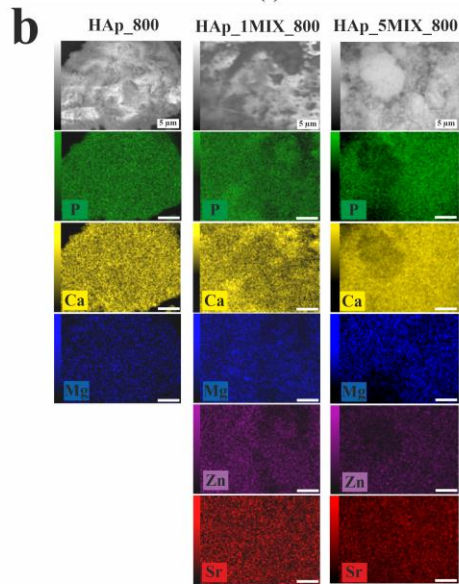
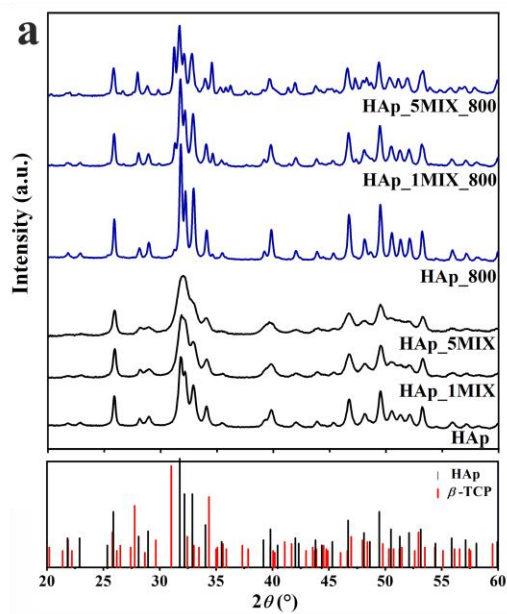


Dr. Antonia Ressler

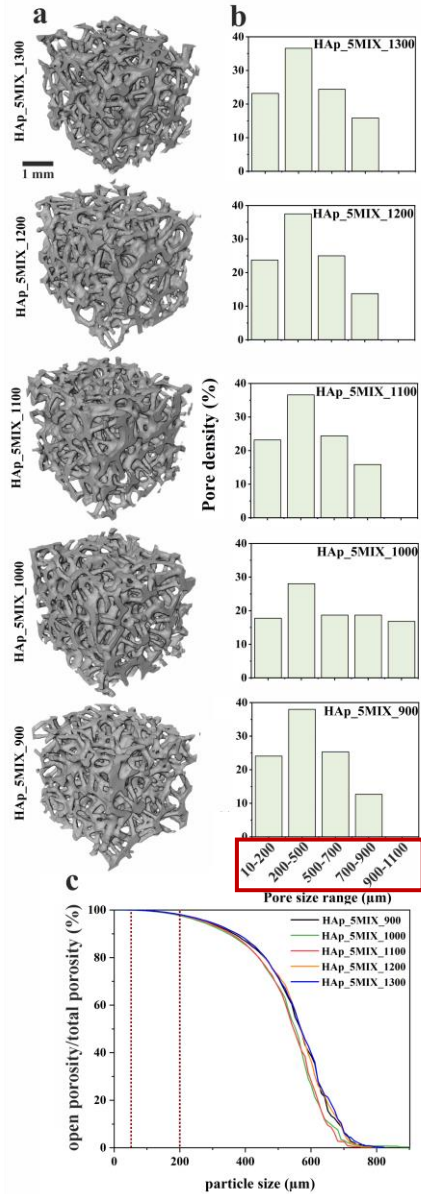
Vat photopolymerization of biomimetic bone scaffolds based on Mg, Sr, Zn-substituted hydroxyapatite: Effect of sintering temperature

Antonia Ressler ^a ✉, Setareh Zakeri ^a ✉, Joana Dias ^b ✉, Markus Hannula ^c ✉,
Jari Hyttinen ^c ✉, Hrvoje Ivanković ^d ✉, Marica Ivanković ^d ✉,
Susanna Miettinen ^{c e} ✉, Martin Schwentenwein ^b ✉, Erkki Levänen ^a ✉,
Erkka J. Frankberg ^a ✉





- Studies have shown that biphasic CaP systems composed of HAp and β -TCP are promising alternatives for achieving materials with improved biodegradation.

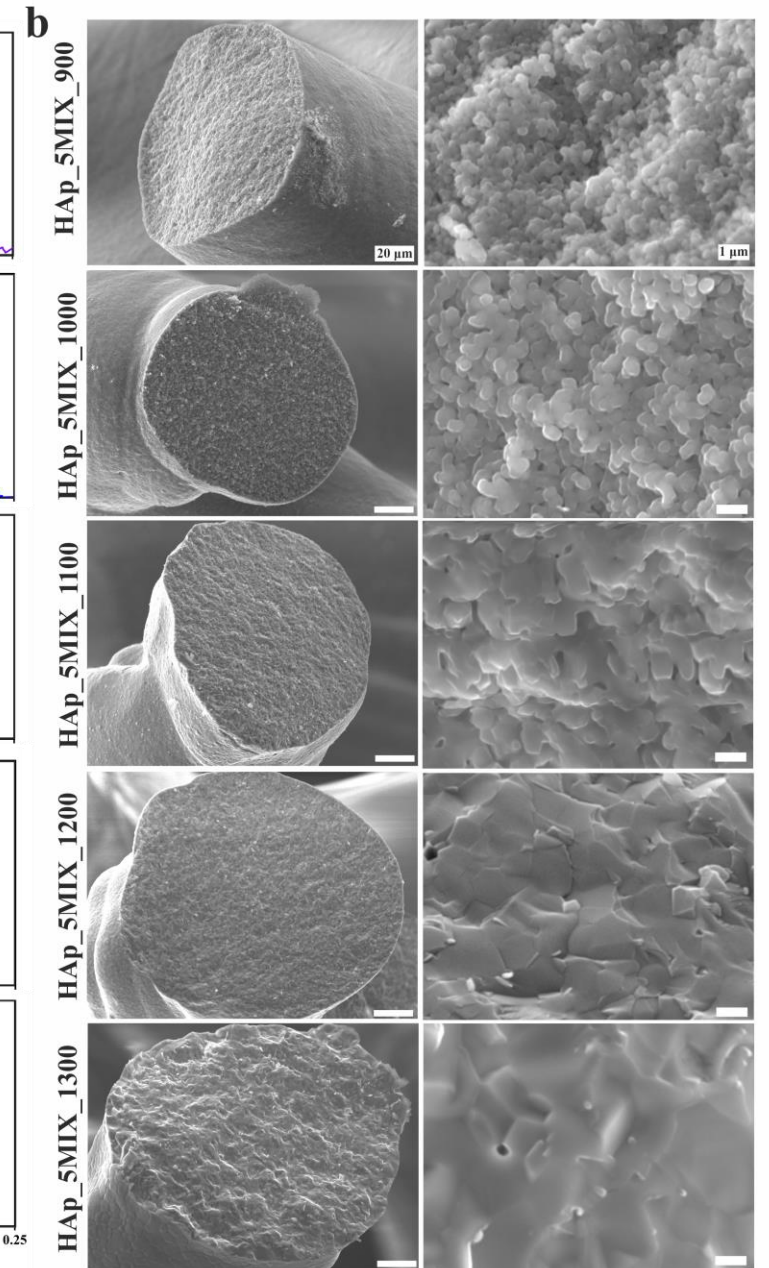
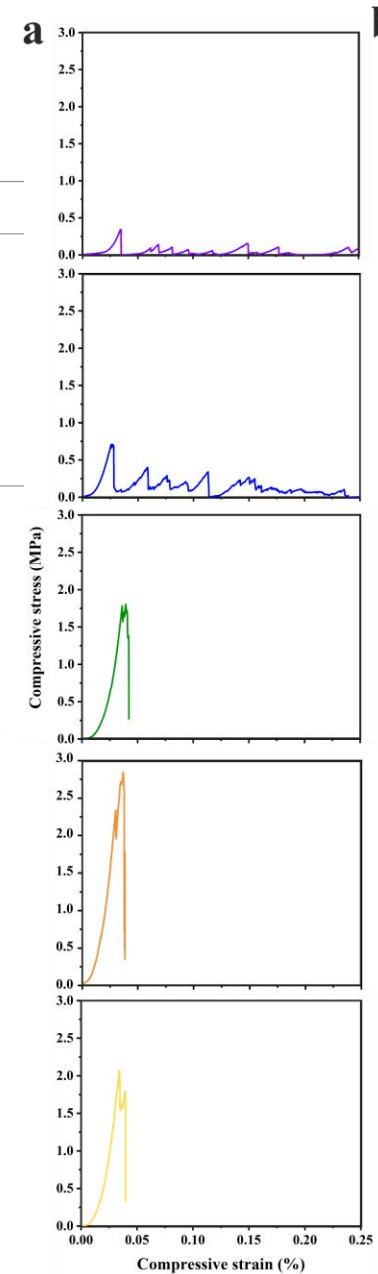


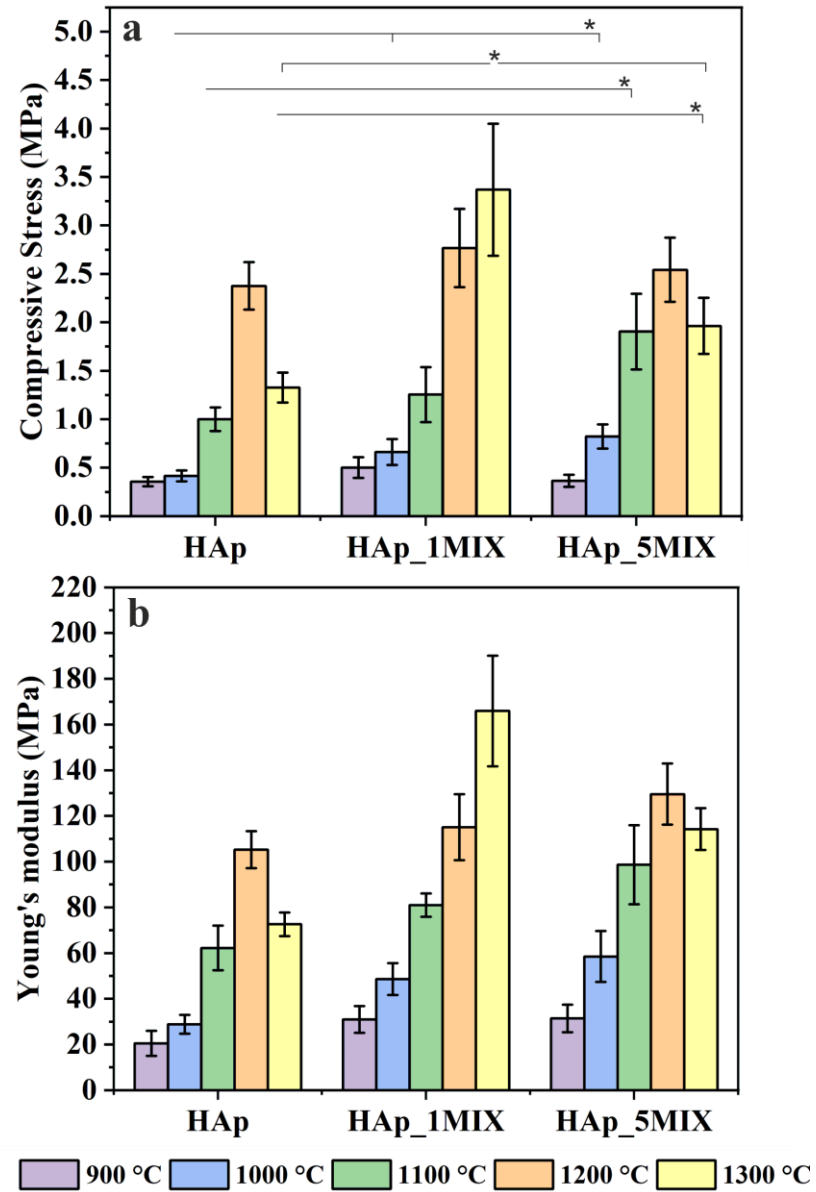
scaffold	porosity (%)	average pore size (μm)	wall thickness (μm)
HAp_5MIX_900	75.55	551.94 \pm 133.55	216.16 \pm 52.81
HAp_5MIX_1000	74.83	536.05 \pm 135.45	214.59 \pm 52.31
HAp_5MIX_1100	75.54	532.79 \pm 126.94	208.24 \pm 55.60
HAp_5MIX_1200	77.43	554.54 \pm 131.01	201.21 \pm 48.98
HAp_5MIX_1300	77.84	555.93 \pm 133.41	194.93 \pm 42.33

The size of mesenchymal stem cells is in the range of 15–30 μm . Particle sizes up to 200 μm are of primary relevance. This size range allows migration of small cell aggregates in the seeding process.

-50 μm particle is able to infiltrate into all pores in fabricated scaffolds

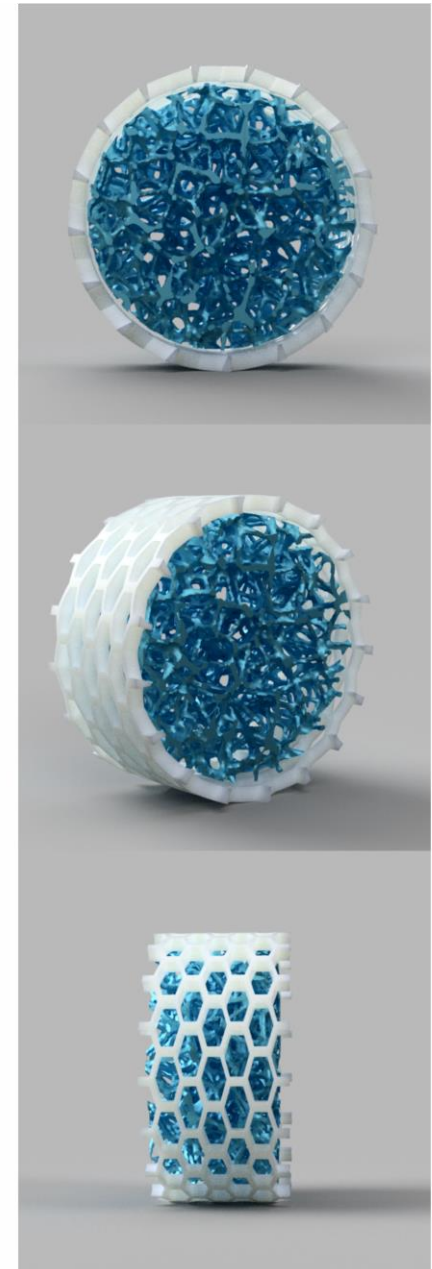
-200 μm particle is able to infiltrate into 98 % of the pores





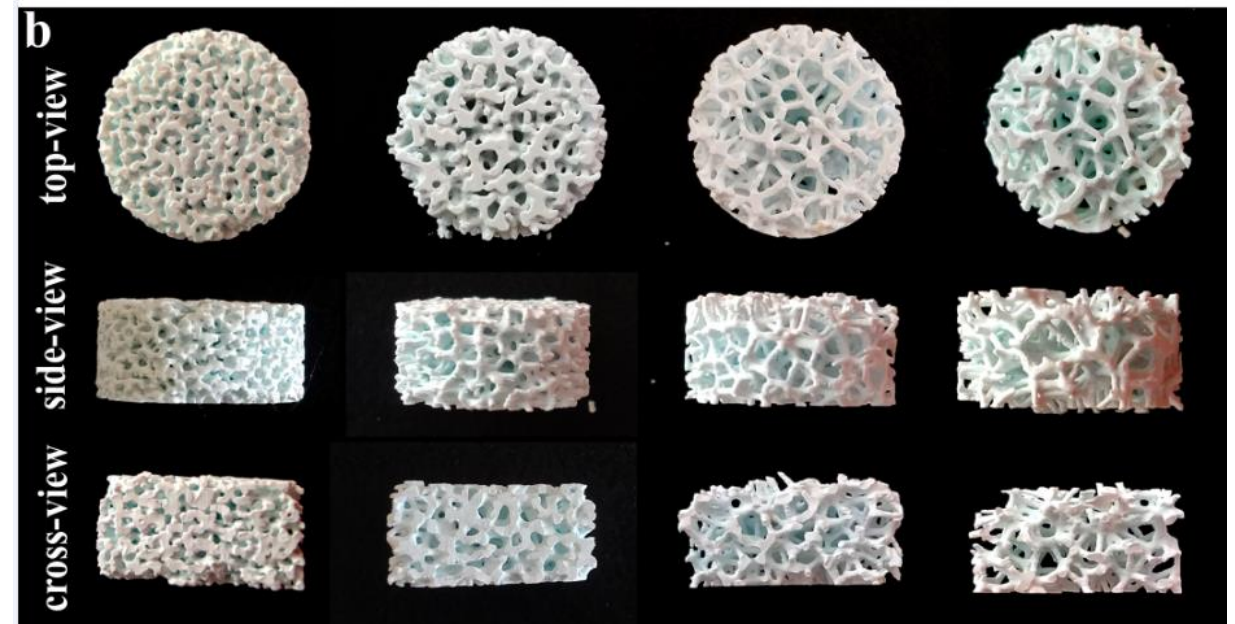
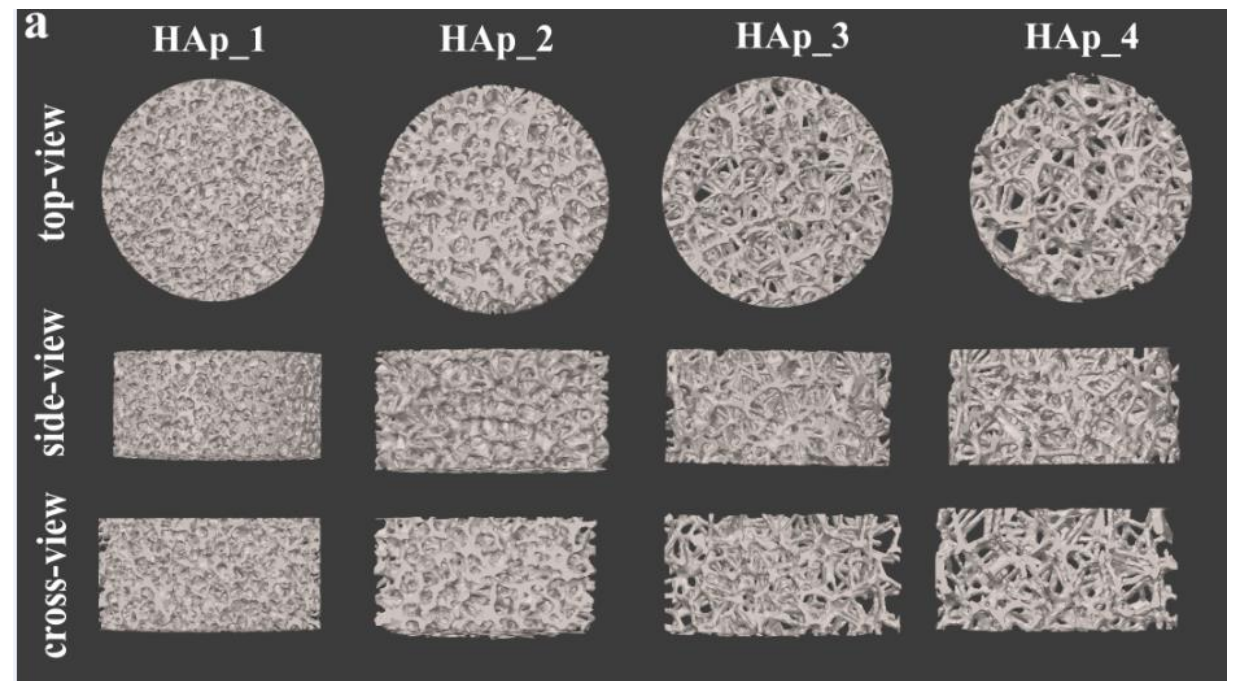
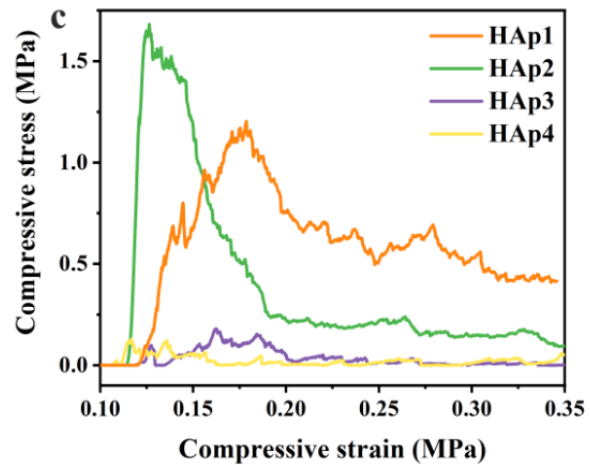
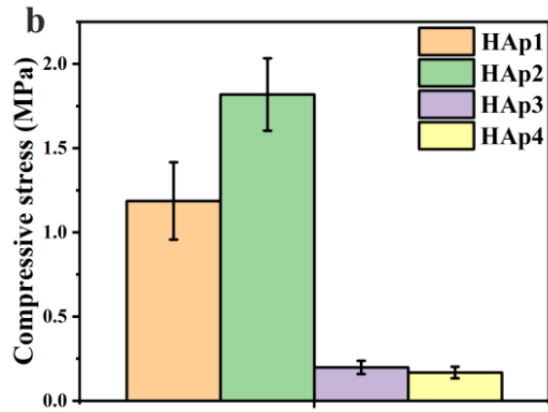
It is worth noting that the mechanical properties of bone exhibit a wide range of reported values, influenced by factors such as local tissue density and testing conditions.

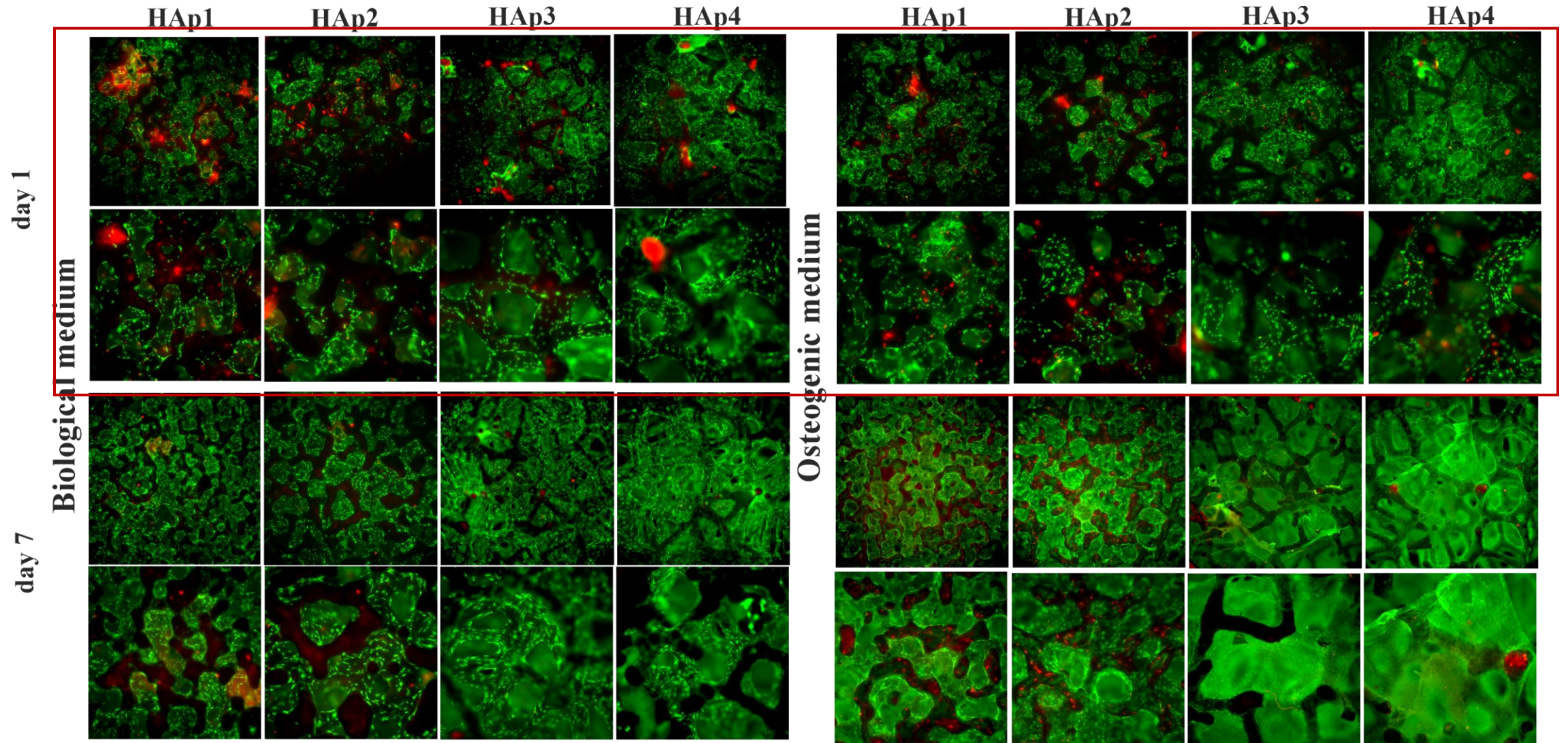
Cancellous (trabecular) bone exhibits the Young's modulus in the range of 0.1–1.0 GPa and the strength that varies from 1 to 10 MPa.

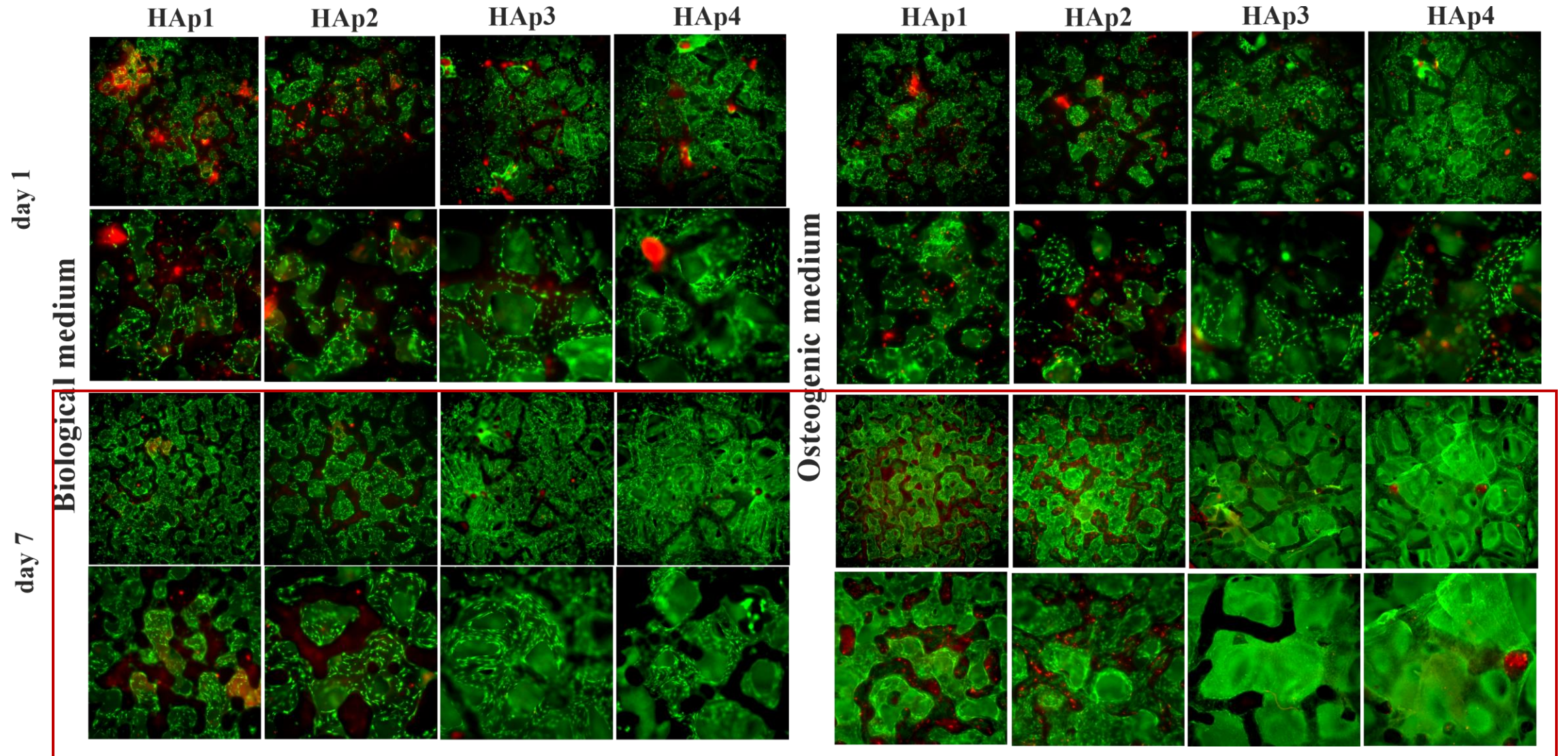


Effect of pore size and porosity

scaffold	porosity (%)	average pore size (μm)	wall thickness (μm)
HAp1	42.930	267.643	291.965
HAp2	45.605	396.535	354.771
HAp3	76.749	707.331	260.536
HAp4	78.701	850.795	292.394

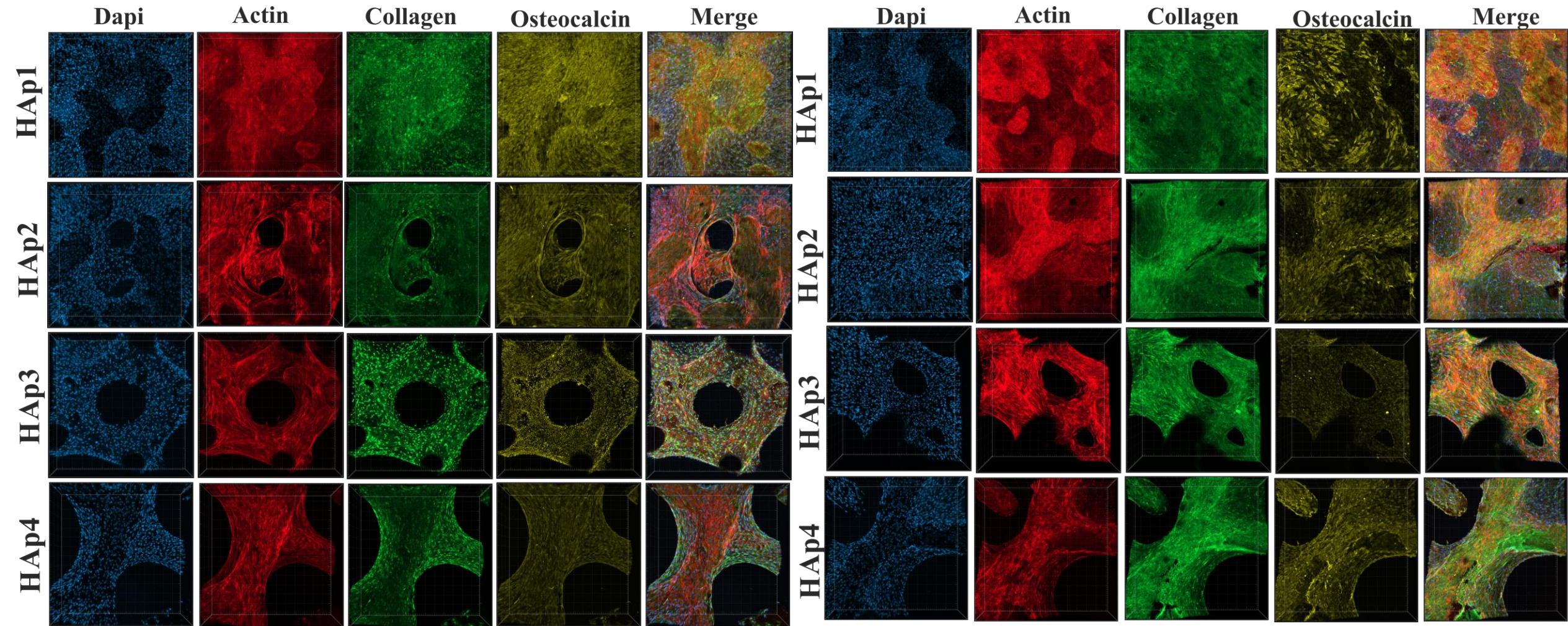


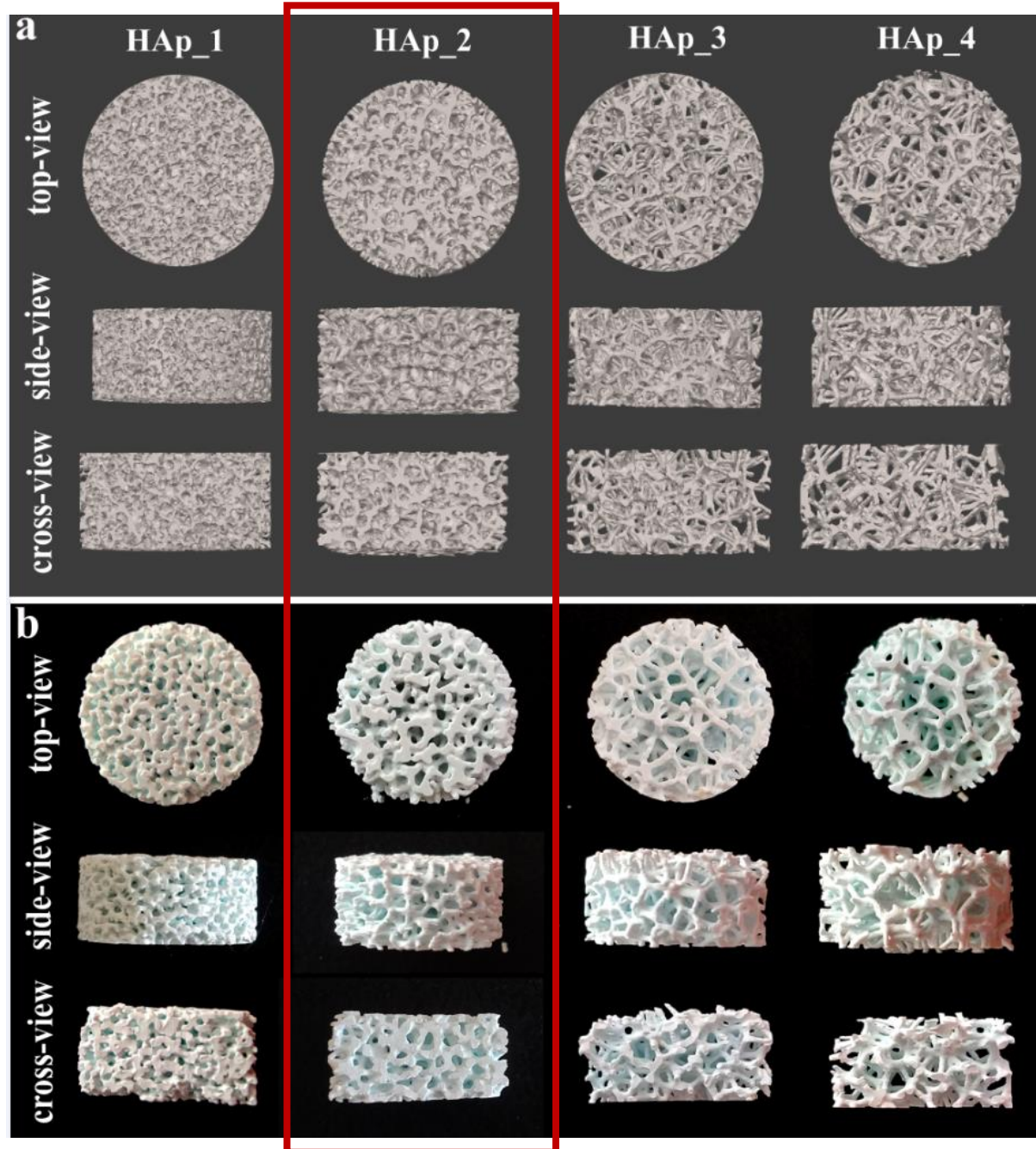




day 14

day 21

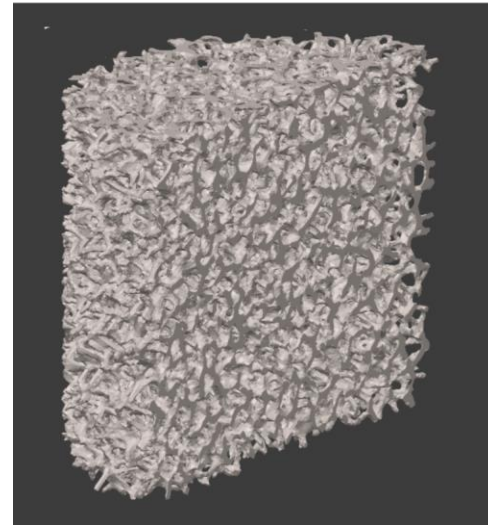




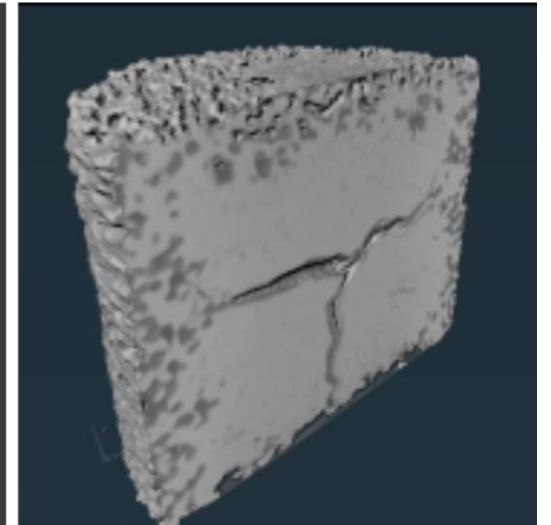
Cleaning challenge of porous scaffolds

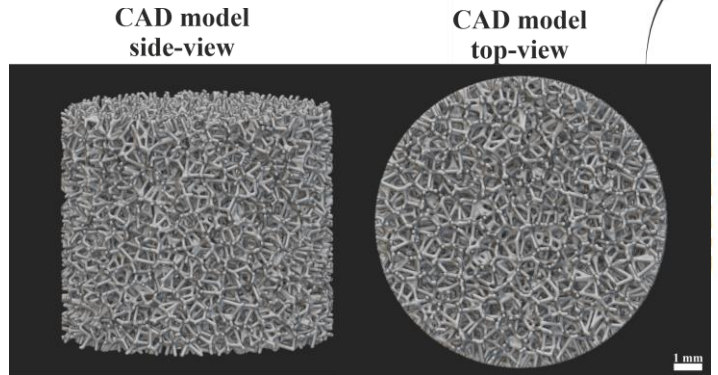
- porous structures where the interconnected pores are intentionally designed to remain uncured
- the uncured slurry in these porous regions can become intricately trapped between the cured layers, complicating the cleaning process
- effectively removing the uncured slurry from within the intricate and porous geometries of the printed structures becomes a critical task as the presence of residue within the structure can obstruct pores during sintering
- biomedical implants \longrightarrow pore characteristics are crucial for tissue integration and substance exchange.

**CAD model
cross section**

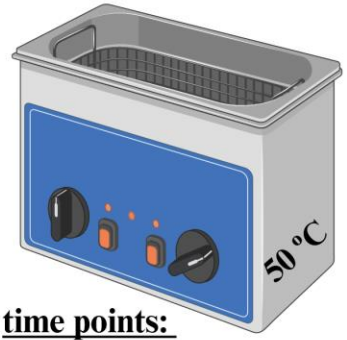


**micro-CT
cross section**





ultrasonic cleaning

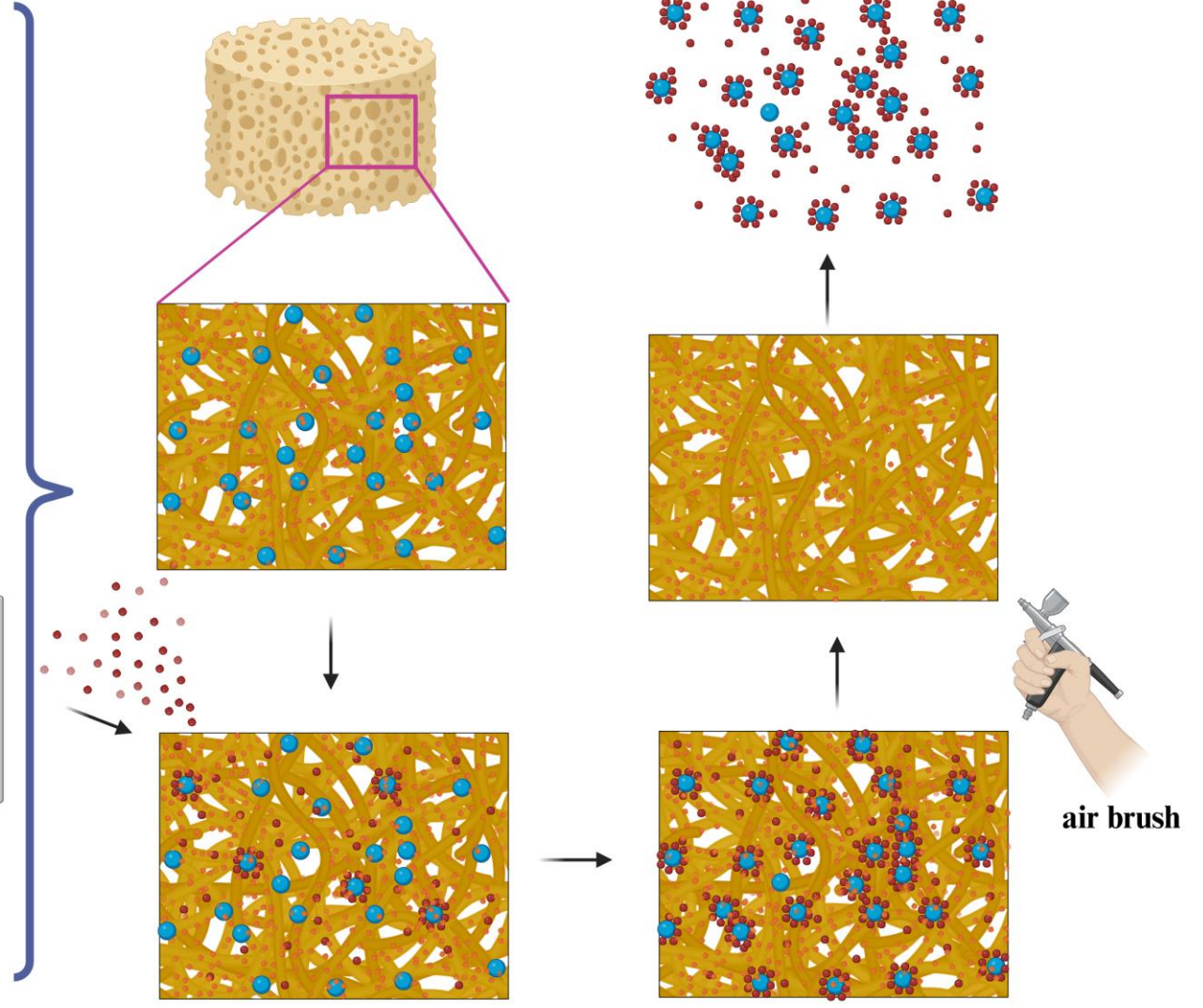


time points:
5, 15 and 30 min,
1, 2, 3 and 4 h

soaking cleaning

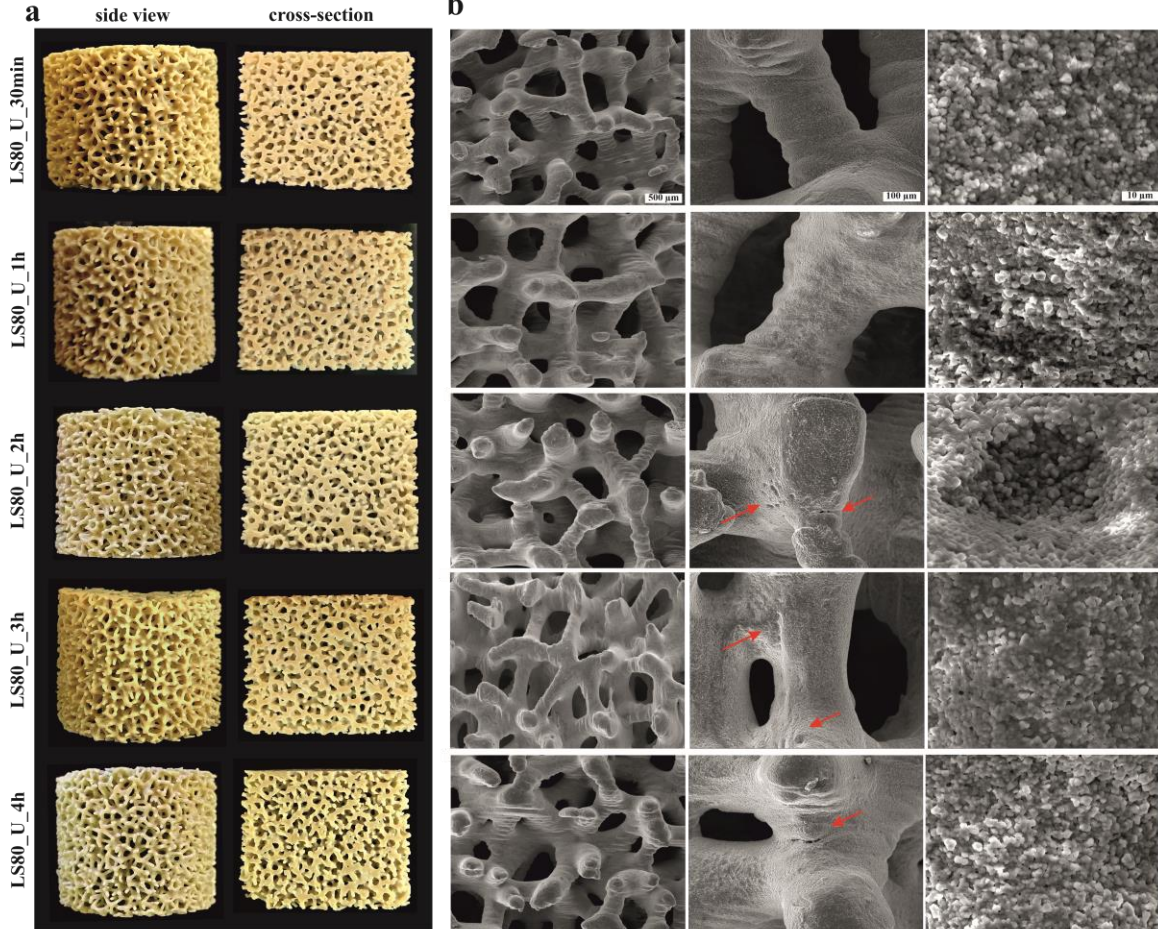


time points:
48, 72 and 96 h

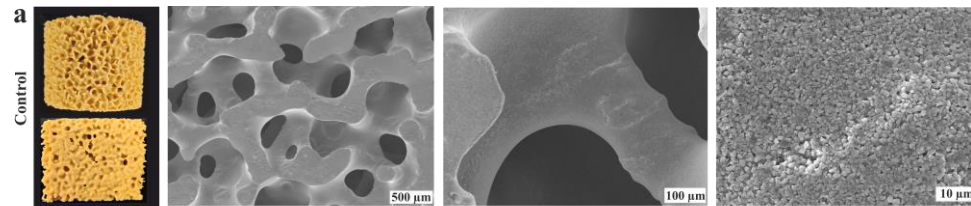
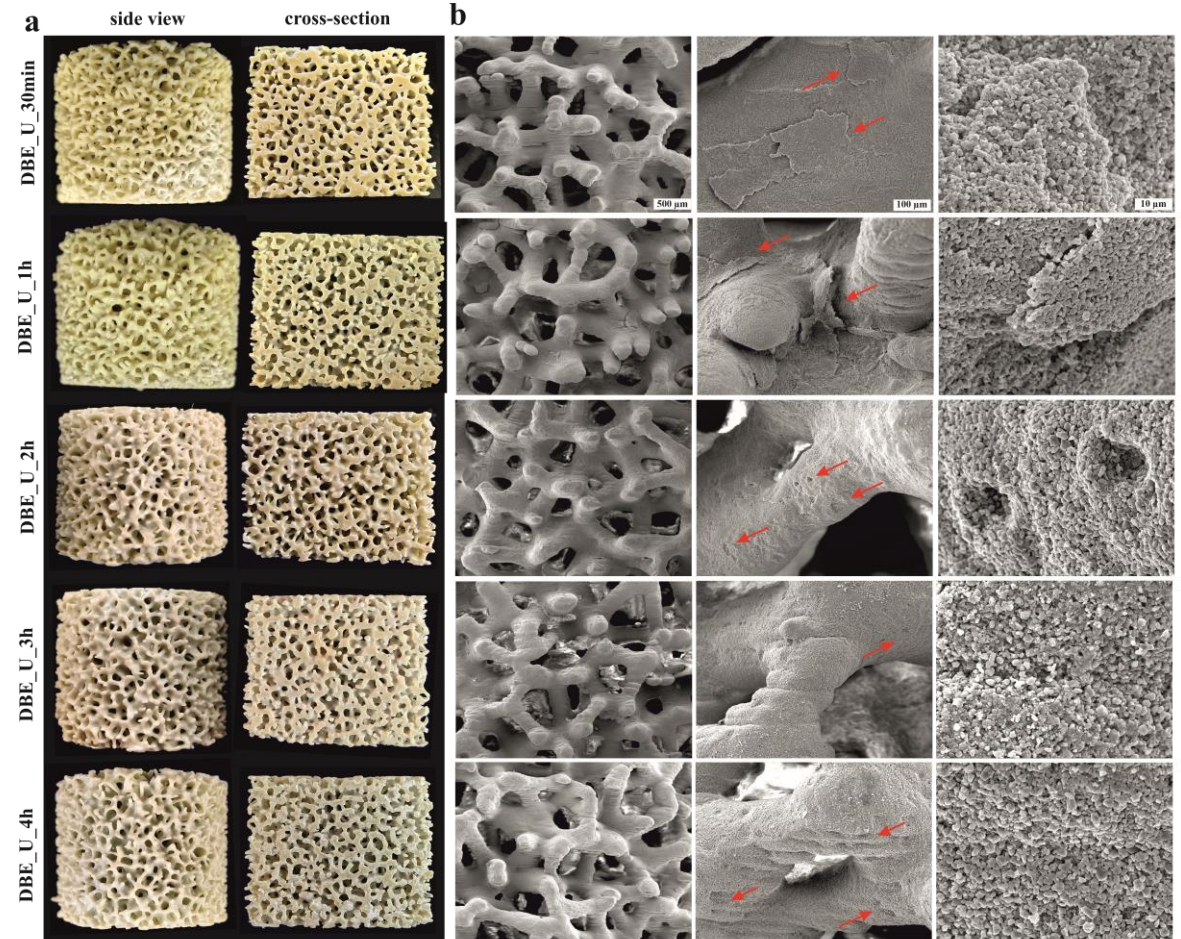


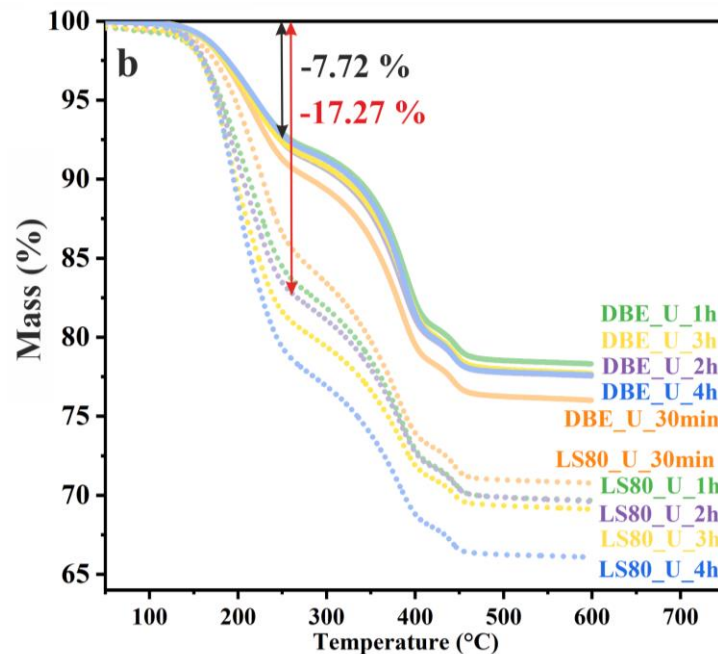
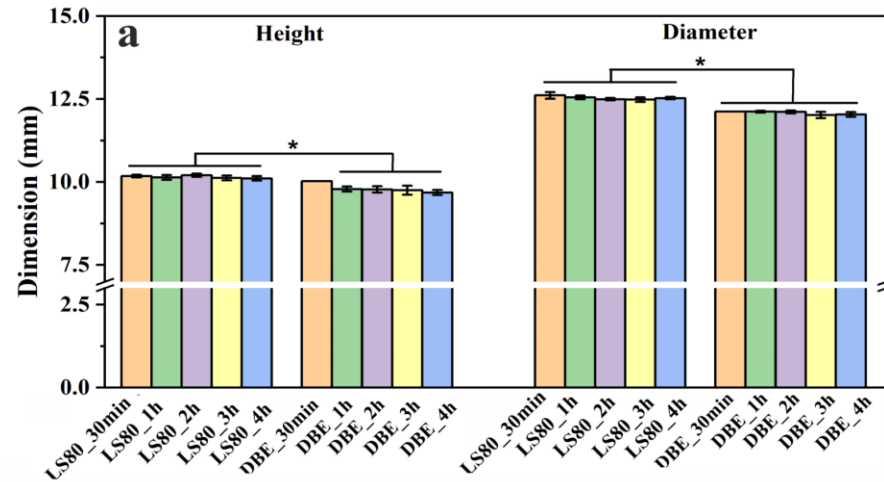
 polymerized scaffold part
  uncured polymer resin
  ceramic (HAp) particle
  LitaSol80 / DBE

LithaSol 80



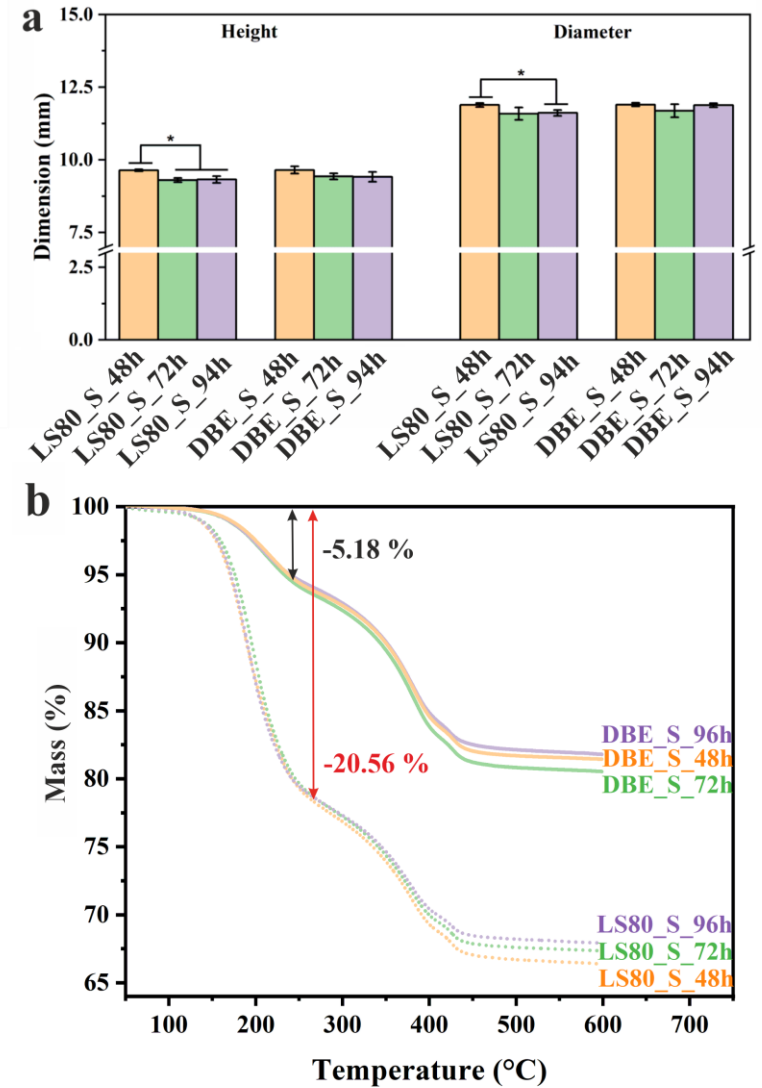
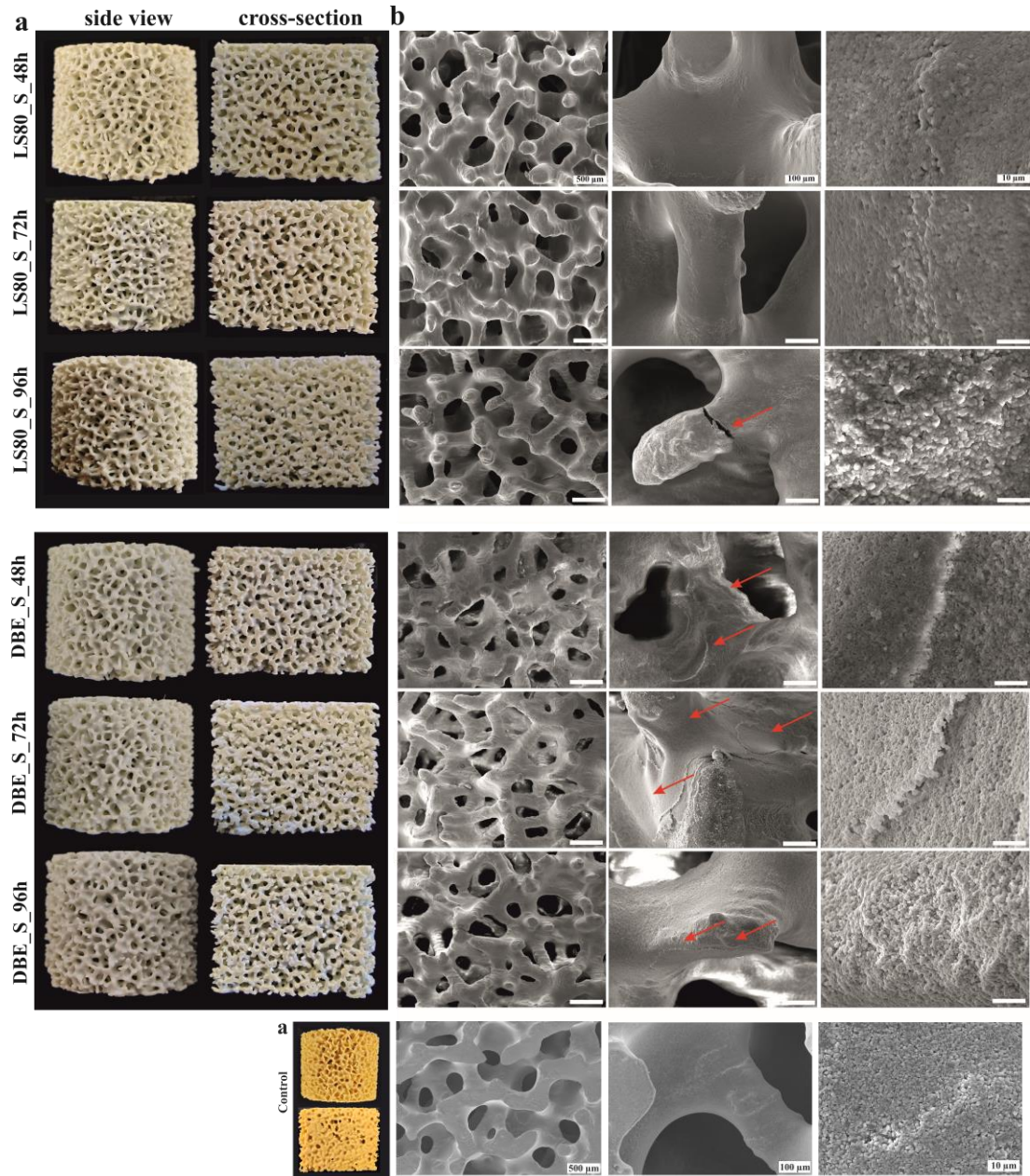
DBE



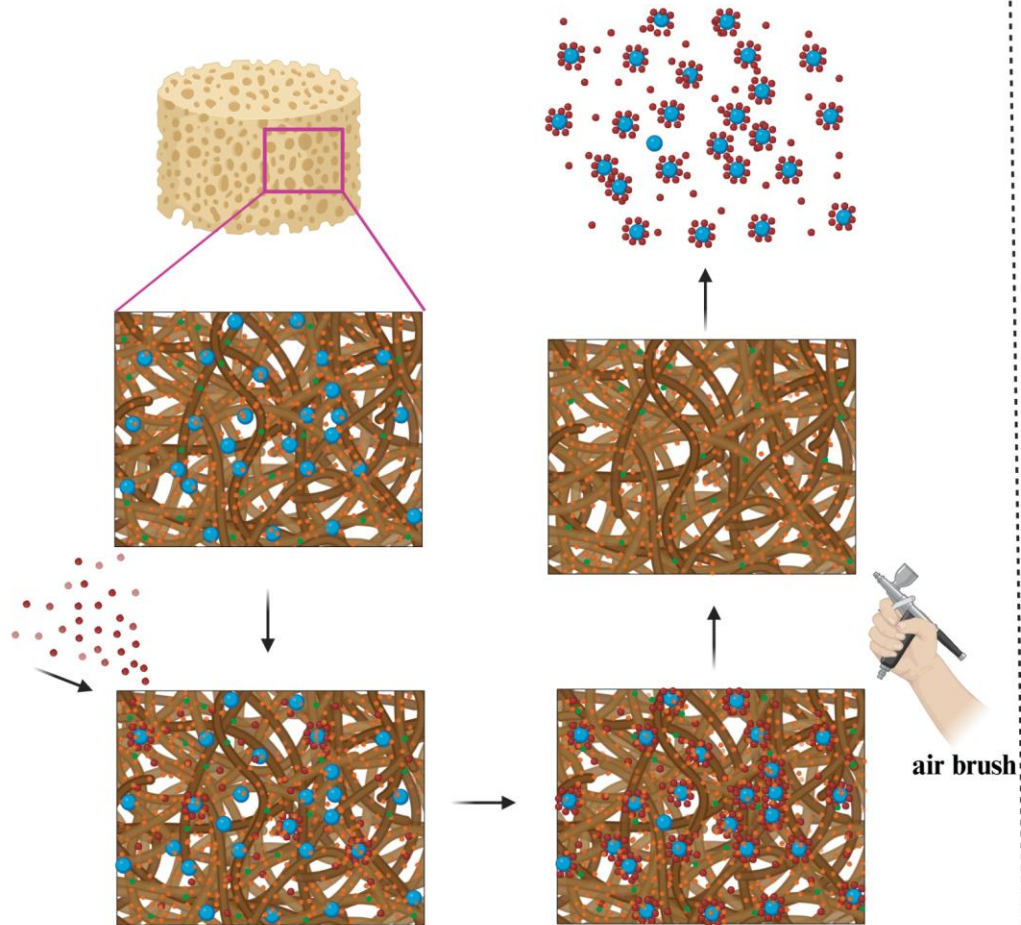


- mass loss started at approximately 150 °C, primarily attributed to the diffusion and evaporation of additives, unreactive diluents and uncured slurry
- the degradation of the major cured organic components initiated around 250 °C
- the significant contrast in the TG curves between scaffolds treated with LithaSol 80 and DBE primarily lies in the initial stage of weight loss
- the observed difference in total mass loss (14.15%) between samples treated with Lithasol 80 and DBE implies the potential occurrence of chemical debinding during cleaning with DBE. However, further detailed examination is required to provide conclusive evidence

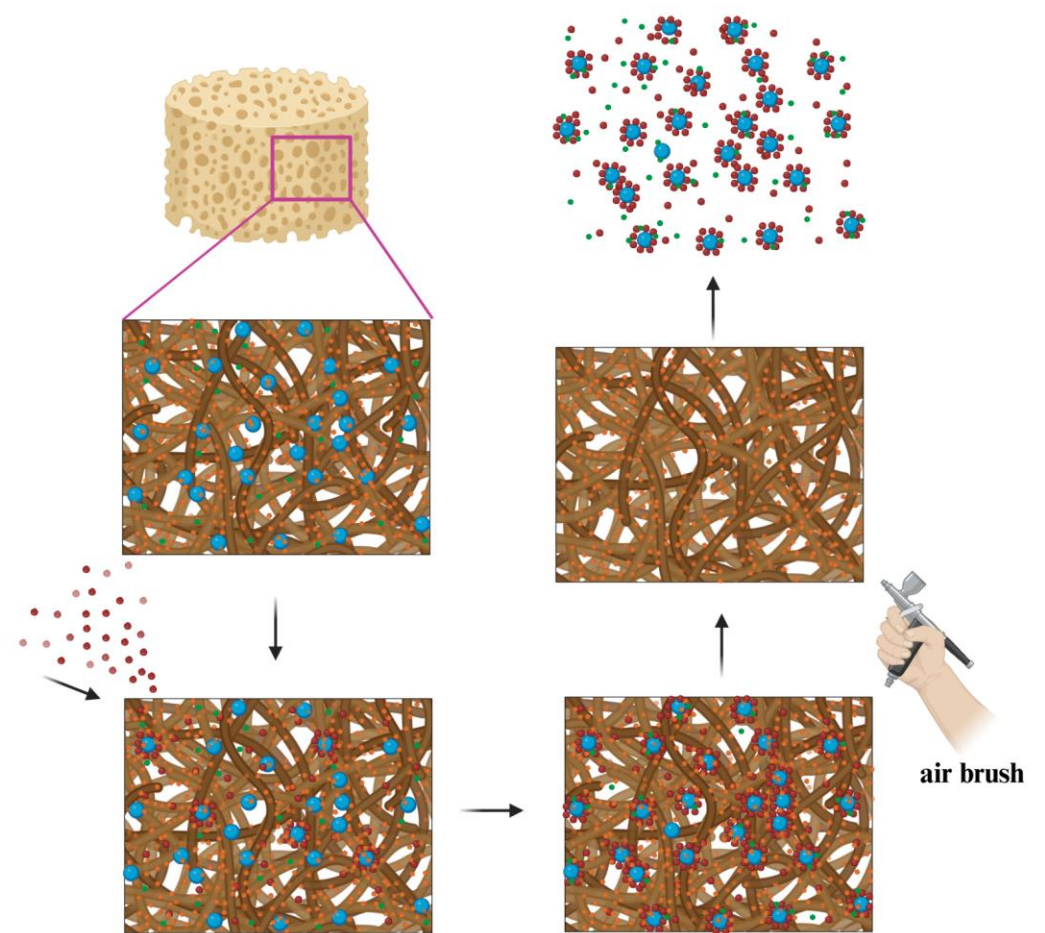
Morphological characterization - soaking








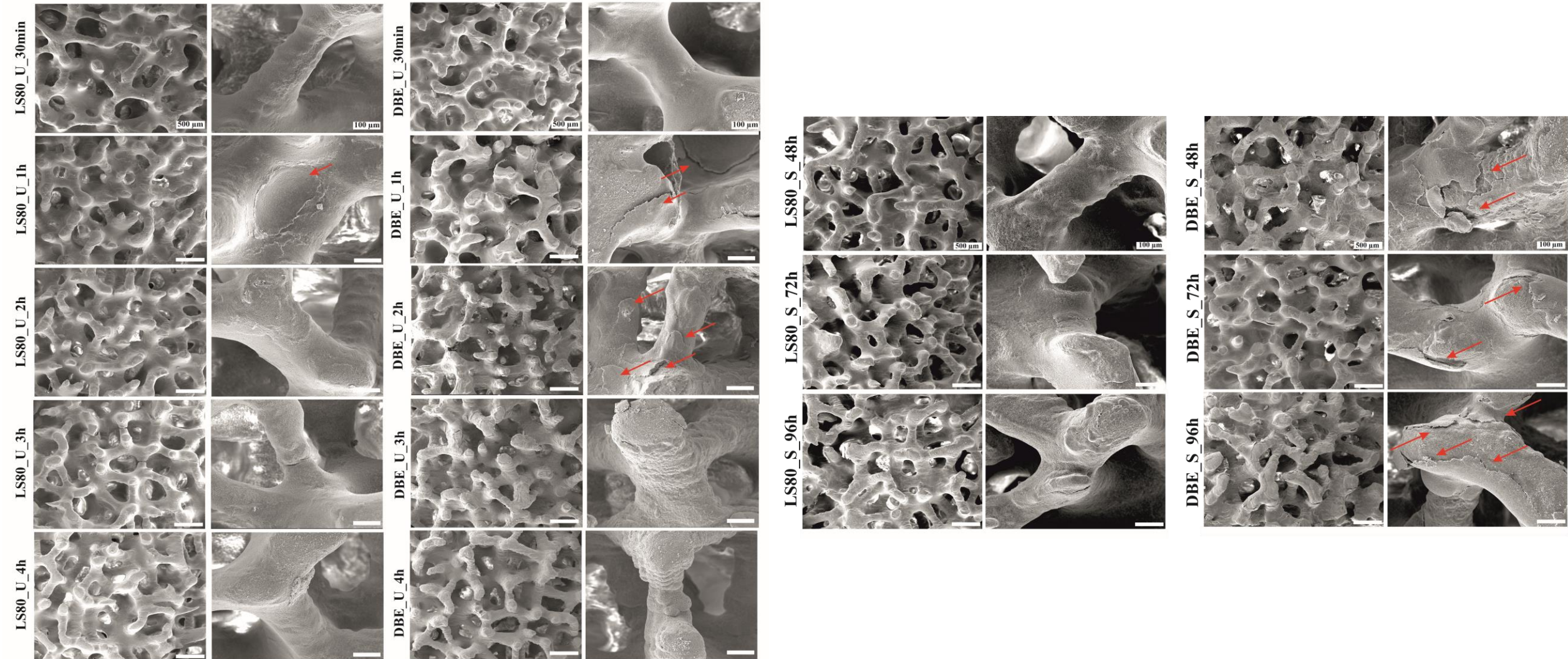
LithaSol 80 cleaning mechanism



DBE cleaning mechanism



 polymerized scaffold part
  uncured polymer resin
  ceramic (HAp) particle
  LithaSol80 / DBE
  additives and unreactive diluents



Conclusion...

Thank you for your attention!

antonia.ressler@tuni.fi